

Effect of Reionization on Structure Formation in the Universe

Nickolay Y. Gnedin

CASA, University of Colorado, Boulder, CO 80309; e-mail: gnedin@casa.colorado.edu

ABSTRACT

I use simulations of cosmological reionization to quantify the effect of photoionization on the gas fraction in low mass objects, in particular the characteristic mass scale below which the gas fraction is reduced compared to the universal value. I show that this characteristic scale can be up to an order of magnitude lower than the linear theory Jeans mass, and that even if one defines the Jeans mass at a higher overdensity, it does not track the evolution of this characteristic suppression mass. Instead, the filtering mass, which corresponds directly to the scale over which baryonic perturbations are smoothed in linear perturbation theory, provides a remarkably good fit to the characteristic mass scale. Thus, it appears that the effect of reionization on structure formation in both the linear and nonlinear regimes is described by a single characteristic scale, the filtering scale of baryonic perturbations. In contrast to the Jeans mass, the filtering mass depends on the full thermal history of the gas instead of the instantaneous value of the sound speed, so it accounts for the finite time required for pressure to influence the gas distribution in the expanding universe. In addition to the characteristic suppression mass, I study the full shape of the probability distribution to find an object with a given gas mass among all the objects with the same total mass, and I show that the numerical results can be described by a simple fitting formula that again depends only on the filtering mass. This simple description of the probability distribution may be useful for semi-analytical modeling of structure formation in the early universe.

Subject headings: cosmology: theory - cosmology: large-scale structure of universe - galaxies: formation - galaxies: intergalactic medium

1. Introduction

The effect of cosmological reionization on the formation and evolution of low mass objects has been under the scrutiny of theorists for a long time, ever since Ikeuchi (1986) and Rees (1986) independently pointed out that the increase in the temperature of the cosmic gas during reionization will suppress the formation of small galaxies with masses below the Jeans mass. Several attempts to quantify the effect of reionization on low mass galaxies have been made since using semi-analytical calculations (Babul & Rees 1992; Efstathiou 1992; Shapiro, Giroux, & Babul

Table 1. Simulation Parameters

Run	N	Box size	Baryonic mass res.	Total mass res.	Spatial res.
A	128^3	$4h^{-1}$ Mpc	$10^{5.7} M_\odot$	$10^{6.6} M_\odot$	$1.0h^{-1}$ kpc
B	128^3	$2h^{-1}$ Mpc	$10^{4.8} M_\odot$	$10^{5.7} M_\odot$	$0.5h^{-1}$ kpc

1994), spherically symmetric modeling (Haiman, Thoul, & Loeb 1996; Thoul & Weinberg 1996), and three-dimensional cosmological hydrodynamic simulations (Quinn, Katz, & Efstathiou 1996; Weinberg, Hernquist, & Katz 1997; Navarro & Steinmetz 1997).

While confirming the general proposition that reionization suppresses formation of low mass galaxies, these studies do not give the full description of the impact of reionization on the gas fraction in the low mass objects. Particularly, one can expect that the effect of reionization depends on the reionization history, and thus is not universal at a given redshift.

Thus, it would be useful to attempt to quantify the effect of reionization on the formation and evolution of the low-mass objects in a more complete manner, relating the effective mass below which an object is a subject to reionization feedback to the characteristic scales present at each given moment of time.

This paper attempts to accomplish precisely that based on the new simulations of cosmological reionization. The simulations of a representative Cold Dark Matter cosmological model¹ were performed with the “Softened Lagrangian Hydrodynamics” (SLH-P³M) code (Gnedin 1995, 1996; Gnedin & Bertschinger 1996) and fully described in Gnedin (2000). Table 1 lists two simulations used in this paper. Parameter N gives the number of the dark matter particles; the quasi-Lagrangian baryonic mesh has the same size. Baryonic mass resolution is an average mass of a baryonic cell, and the total mass resolution is the mass of a dark matter particle plus the average mass of a baryonic cell. The spatial resolution is measured as the gravitational softening length (the real resolution of both the gravity solver and the gas dynamics solver is a factor of two worse). Reionization by stars (i.e. with a soft UV background spectrum) is modeled with the Local Optical Depth approach, which is able to approximately follow the three-dimensional radiative transfer in the cosmological density distributions.

The two simulations from Table 1 allow me to investigate the sensitivity of my results to the missing small and large scale power: run A has a larger box whereas run B has a higher resolution. They also have different reionization histories, which allows me to test the generality of my results.

¹With the following cosmological parameters: $\Omega_0 = 0.3$, $\Omega_\Lambda = 0.7$, $h = 0.7$, $\Omega_b = 0.04$, $n = 1$, $\sigma_8 = 0.91$, where the amplitude and the slope of the primordial spectrum are fixed by the COBE and cluster-scale normalizations.

Both simulations have sufficient mass resolution and the box size to resolve the relevant characteristic mass scales during reionization and thus can be used for the purpose of this paper. Since both simulations have box sizes comparable to the nonlinear scale at the present time, they cannot be continued until $z = 0$. Rather, run A is stopped at $z = 4$ and run B at $z = 6.5$.

The goal of this paper is to quantify the relationship between the total mass of an object M_t and its gas mass M_g . The advantage of using the simulations listed in Table 1 is that they have enough resolution (both in mass and space) to actually map the full two-dimensional distribution of objects in the $M_t - M_g$ plane. But before this can be done, I need to discuss what characteristic mass scales are relevant for the evolution of the cosmic gas. This is particularly important because, as the reader is reminded in the next section, the Jeans mass, initially proposed as the characteristic scale, is essentially irrelevant in the expanding universe.

2. Reminder: the Linear Theory

The effect of the reionization of the universe and the associated reheating of the cosmic gas on the evolution of linear perturbations was comprehensively discussed in Gnedin & Hui (1998). As they showed, the relationship between the linear overdensity of the dark matter $\delta_d(t, k)$ and the linear overdensity of the cosmic gas $\delta_b(t, k)$ as a function of time and the comoving wavenumber k , in the limit of small k ($k \rightarrow 0$), can be written as

$$\frac{\delta_b(t, k)}{\delta_d(t, k)} = 1 - \frac{k^2}{k_F^2} + O(k^4), \quad (1)$$

where k_F is in general a function of time. They called the physical scale associated with the comoving wavenumber k_F the *filtering scale*, since it is the characteristic scale over which the baryonic perturbations are smoothed as compared to the dark matter.

The filtering scale is related to the Jeans scale k_J ,

$$k_J \equiv \frac{a}{c_S} \sqrt{4\pi G \bar{\rho}} \quad (2)$$

(here $\bar{\rho}$ is the average total mass density of the universe, c_S is the sound speed, which is uniquely defined in linear theory, and a is the cosmological scale factor), by the following relation:

$$\frac{1}{k_F^2(t)} = \frac{1}{D_+(t)} \int_0^t dt' a^2(t') \frac{\dot{D}_+(t') + 2H(t')\dot{D}_+(t')}{k_J^2(t')} \int_{t'}^t \frac{dt''}{a^2(t'')}, \quad (3)$$

where $D_+(t)$ is the linear growing mode in a given cosmology.

For a flat universe at high redshift $z \gtrsim 2$, the scale factor a is well approximated by the power-law in time, $a \propto t^{2/3}$, and the growing mode D_+ is proportional to a . In this case equation (3) can be substantially simplified:

$$\frac{1}{k_F^2(a)} = \frac{3}{a} \int_0^a \frac{da'}{k_J^2(a')} \left[1 - \left(\frac{a'}{a} \right)^{1/2} \right]. \quad (4)$$

Inspection of equation (3) shows that the filtering scale *as a function of time* is related to the Jeans scale *as a function of time*, but at *a given moment in time* those two scales are unrelated and can be very different. Thus, given the Jeans scale at a specific moment in time, nothing can be said about the scale over which the baryonic perturbations are smoothed. It is only when the whole time evolution of the Jeans scale up to some moment in time is known that can the filtering scale at this moment be uniquely defined.²

The physical explanation of this result is very simple: the gas temperature (and thus the Jeans scale) can increase very quickly, but the gas density distribution can only change on the dynamical time scale, which is about the Hubble time for the linear perturbations. Thus, the effect of the increased pressure on the gas density distribution will be delayed and can only occur over the Hubble time.

While formally the filtering scale is only defined on large scales, as $k \rightarrow 0$, the following formula

$$\frac{\delta_b(t, k)}{\delta_d(t, k)} \approx e^{-k^2/k_F^2} \quad (5)$$

provides a remarkably accurate fit on all scales up to at least $k = k_F$, and is also very accurate when one needs to calculate the integrals over the baryonic power spectrum $P_b(k) = \delta_b(t, k)^2$. There is no obvious physical reason why equation (5) should be a good fit to the full solution of the linear theory equations, but it was extensively tested over a very large region of the parameter space of possible cosmological models and was always found to work well.

Since my task is to compare the baryonic versus the total mass for small objects, it is convenient to switch from spatial to mass scales. In linear theory, of course, there exists a one-to-one relationship between the two. Thus, I can define the Jeans mass,

$$M_J \equiv \frac{4\pi}{3} \bar{\rho} \left(\frac{2\pi a}{k_J} \right)^3,$$

and the filtering mass,

$$M_F \equiv \frac{4\pi}{3} \bar{\rho} \left(\frac{2\pi a}{k_F} \right)^3,$$

as the mass enclosed in the sphere with the comoving radius equal to the corresponding spatial scale. The relationship between the two mass scales for $D_+ \propto a \propto t^{2/3}$ can be easily obtained from equation (4):

$$M_F^{2/3} = \frac{3}{a} \int_0^a da' M_J^{2/3}(a') \left[1 - \left(\frac{a'}{a} \right)^{1/2} \right]. \quad (6)$$

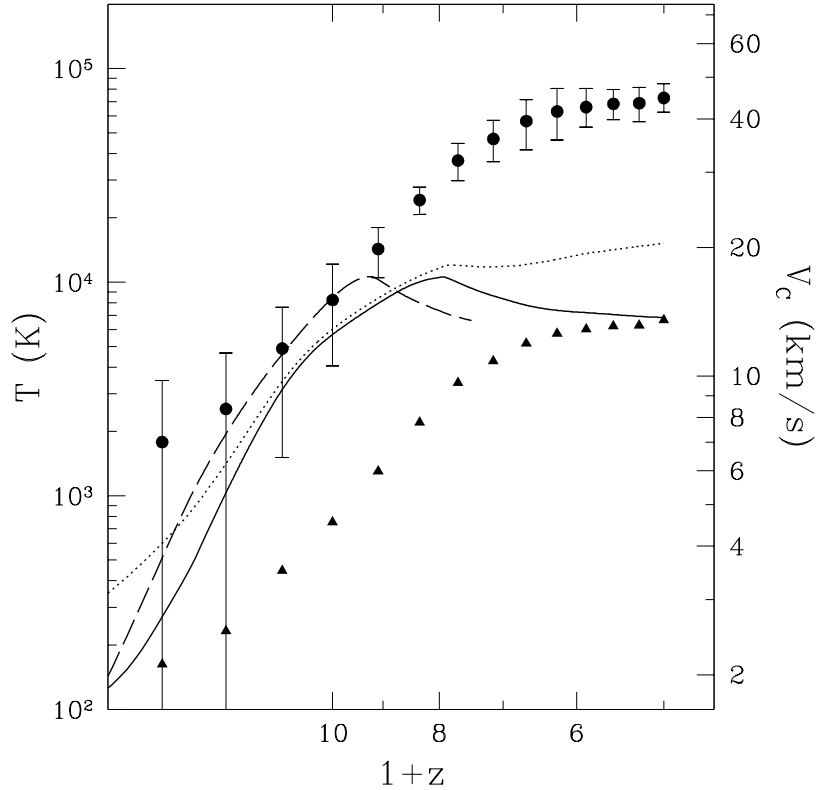


Fig. 1.— The evolution of the mass- (*dotted line*) and volume- (*solid line*) weighted temperature from run A. Also shown is the volume-averaged temperature for run B (*long-dashed line*). The filled circles with error-bars label the virial temperature of objects that on average have the baryonic fraction of 50% of the universal value. The triangles show the Jeans temperature at the virial overdensity of 180 that corresponds to this virial temperature (eq. [9]). The right y axis shows the circular velocity that corresponds to the virial temperature marked by filled circles (the right y axis has no meaning for other curves on this plot).

3. Main Results

Figure 1 shows the evolution of the volume- and mass-weighted temperature in the simulations. Since the gas density and temperature are not uniform in the simulation, the definition of the linear sound speed (or linear temperature) is somewhat ambiguous. I therefore adopt the volume-averaged temperature as a substitute for the linear theory temperature, so that the linear theory sound speed, which enters the definition of the linear theory Jeans mass, is defined as

$$c_S^2 = \frac{5}{3} \frac{k_B \langle T \rangle_V}{\mu m_p},$$

where $\mu = 0.59$ is the mean molecular weight of the fully ionized gas.

²In general it is also true that the filtering scale is equal to the Jeans scale at some earlier moment in time.

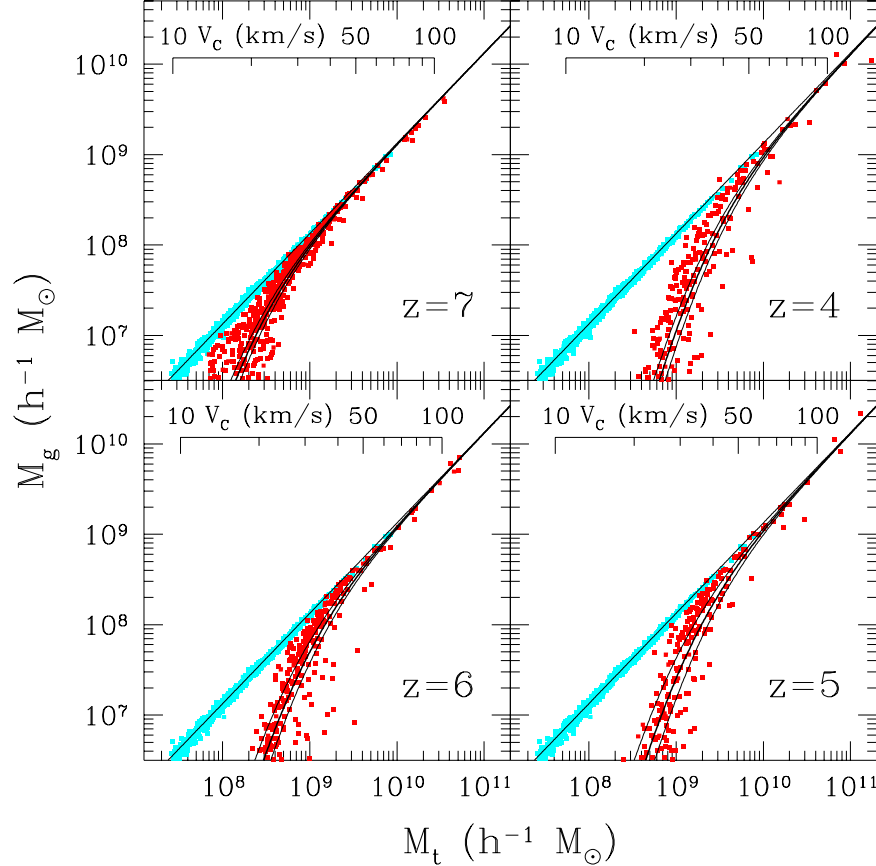


Fig. 2.— The gas versus the total mass for all objects from run A taken at four different redshifts (dark grey points; redshift decreases in the counter-clockwise direction). Also shown with the light grey color the gas versus total mass at $z = 15$. The straight line marks the position of the universal baryon fraction, $M_g = (\Omega_b/\Omega_0)M_t$, and three curved lines show the fit to the function $\bar{M}_g(M_t)$ together with 95% confidence levels. The inserted axes show the circular velocity corresponding to the total mass at each redshift.

However, the specific definition of the linear sound speed is not very important. For example, if I used the mass-weighted mean temperatures instead of the volume-weighted one, or instead, I calculate the mass- or volume-weighted Jeans mass directly from the simulation, the difference in the computed Jeans and filtering masses would be smaller than the statistical uncertainty due to a finite number of objects in my simulation (i.e. smaller than the error-bars in Fig. 3).

The relationship between the gas and the total mass of cosmological objects in the simulations is now shown in Figure 2.³ Bound objects are identified using the DENMAX algorithm of Bertschinger & Gelb (1991) with the gaussian density smoothing length equal to one fifth of the mean interparticle separation, which corresponds to the characteristic overdensity of about 100.

³In all cases the stellar mass makes only a small correction to the total gas mass and is ignored.

Before reionization ($z = 15$, light grey color) the gas mass is directly proportional to the total mass of all objects, and the coefficient of proportionality is the universal baryon fraction $f_b \equiv \Omega_b/\Omega_0$. In the simulation shown (run A) reionization occurs at $z \approx 7$, and at that redshift the effects of reheating start to appear. As time progresses, larger and larger mass objects are affected by the increase in the gas temperature.

Without additional analysis, it is impossible to say whether the reduction of the gas mass in low mass objects is due to the expulsion of the already accreted gas, or due to the suppression of the accretion. It is likely that both effects play a role - for example, essentially all objects with masses below $2 \times 10^8 M_\odot$ lost their gas between $z = 7$ and $z = 6$, and since the average mass of a cosmological object does not increase significantly during this short time interval, it is clear that the gas was expelled from the low-mass objects.

The first quantity of interest is the average baryonic mass of all objects with given total mass, $\overline{M}_g(M_t)$. This quantity would be useful for semi-analytical modeling since it can be directly plugged into the Press-Schechter approximation. Before reionization this function has a very simple form, $\overline{M}_g = f_b M_t$, but after reionization the small mass end of \overline{M}_g is suppressed. In order to obtain a practically useful result, I approximate the mean baryonic mass with the following fitting formula,

$$\overline{M}_g = \frac{f_b M_t}{[1 + (2^{1/3} - 1) M_C / M_t]^3}, \quad (7)$$

which depends on a single parameter - the characteristic mass M_C , which is the total mass of objects that on average retain 50% of their gas mass.

In order to measure M_C from the simulation, I first measure the average gas mass and its error-bars as a function of the total mass from the simulation by averaging the gas mass of all objects within 0.1 dex around the given value of the total mass. Then the value of M_C and the corresponding error-bars are found by a standard χ^2 minimization.

The rationale for the particular choice of the fitting function is the following: it is clear from Fig. 2 that at small masses the mean baryonic mass goes as M_t^4 . I have therefore tried fitting formulae of the following kind,

$$\overline{M}_g = \frac{f_b M_t}{[1 + (2^{\alpha/3} - 1) (M_C / M_t)^\alpha]^{3/\alpha}},$$

and $\alpha = 1$ gives the best values for the χ^2 test over the whole time evolution.⁴

Figure 3 now shows the evolution of the Jeans mass M_J , the filtering mass M_F , and the characteristic mass M_C for both simulations. One can immediately see that the filtering mass

⁴At selected moments in time an equally good fit can be obtained with different α . For example, at $z = 4$, $\alpha = 2$ gives as good a fit as $\alpha = 1$. By eye it appears that $\alpha = 2$ might be better than $\alpha = 1$, but this appearance is misleading; Fig. 2 is shown on log-log scale, while \overline{M}_g is the average mass, and not the exponent of the average logarithm of mass.

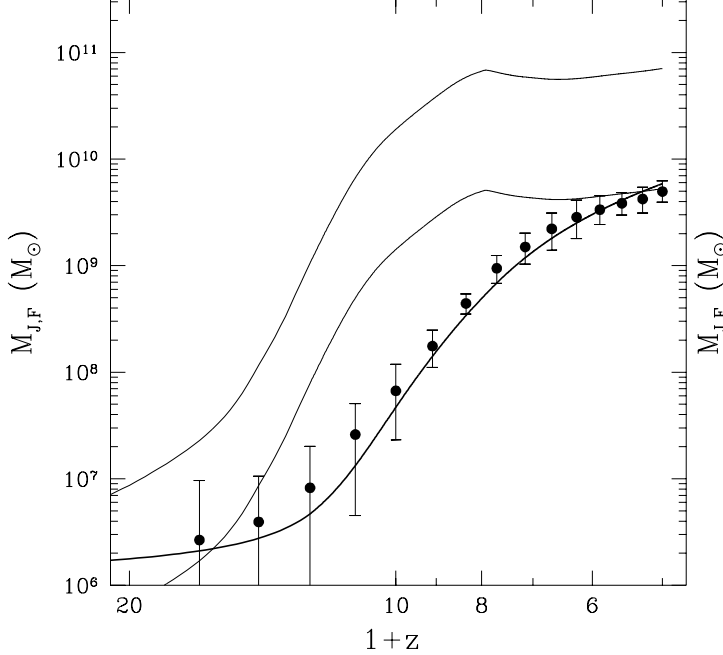


Fig. 3a

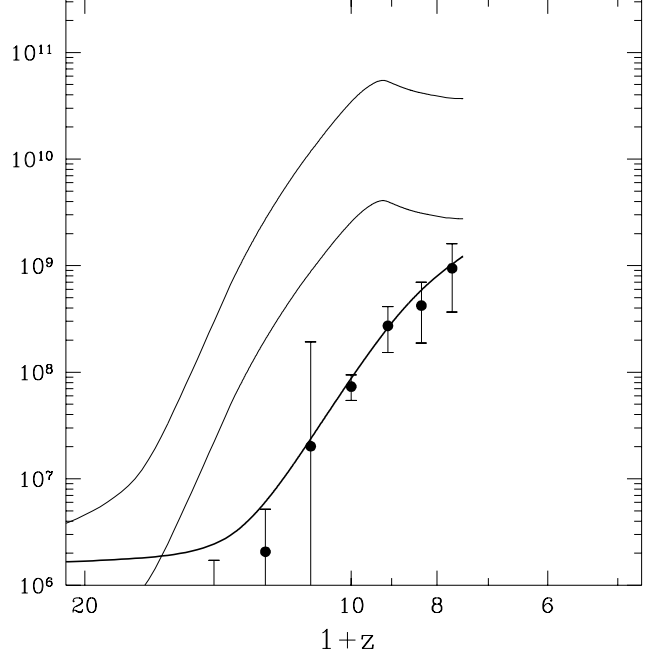


Fig. 3b

Fig. 3.— The evolution of various mass scales for two simulations: run A (a) and run B (b). The two thin lines show from the top down the linear theory Jeans mass (M_J) and the Jeans mass at the virial overdensity of 180 ($M_J/\sqrt{180}$). The bold line shows the filtering mass (M_F), and the symbols with error-bars show the characteristic mass M_C at which $\bar{M}_g = 0.5f_b M_t$, as measured from the simulations.

provides a good fit for the characteristic mass M_C , whereas the linear theory Jeans mass is much larger. One could, however, argue that the linear theory Jeans mass is the wrong scale to use, and that the Jeans mass at the virial overdensity $1 + \delta = 18\pi^2$ should be used instead. The lower thin line shows the virial overdensity Jeans mass, which provides a good fit to the characteristic scale at the end of run A. However, and this is the most important point of this paper, *the overall shape is wrong*, which indicates that the agreement between the Jeans mass at the virial density and the characteristic mass scale at $z \sim 4$ is a mere coincidence. Rather, a linear theory filtering mass should be used as an approximation to the characteristic mass M_C ,

$$\bar{M}_g(M_t, t) \approx \frac{f_b M_t}{[1 + (2^{1/3} - 1)M_F(t)/M_t]^3}. \quad (8)$$

This result can also be cast in the temperature units. The circles with the error-bars in Fig. 1 show the virial temperature,

$$T_{\text{vir}} \equiv \frac{\mu m_p v_c^2}{2k_B} = \frac{\mu m_p G M_t^{2/3} (3\pi^3 \bar{\rho})^{1/3}}{k_B}$$

(Thoul & Weinberg 1996) that corresponds to the characteristic mass M_C for run A (the right y axis shows the respective circular velocity). The same mass corresponds to the Jeans mass at the

virial overdensity for gas with the temperature of

$$T_J \equiv \frac{\mu m_p}{k_B} \frac{3^{7/3}}{10\pi} GM^{2/3} \bar{\rho}^{1/3} = \frac{9}{10\pi^2} T_{\text{vir}}. \quad (9)$$

The value of T_J is shown in Fig. 1 with the filled triangles. Thus, if one wants to use the Jeans mass at the virial overdensity to quantify the effect of reionization on structure formation, one must use the effective temperature T_{eff} of reheated gas so that $M_{J,\text{eff}} = M_F$, which in terms of temperature translates into $T_{\text{eff}} \sim 8 \times 10^3$ K at $z \sim 4$ and $T_{\text{eff}} \sim 2 \times 10^3$ K during reionization, rather than $T_{\text{eff}} = (1 - 2) \times 10^4$ K at all times.

Thus, the effect of the expansion of the universe (which causes the delay of the growth of the filtering mass M_F with respect to the linear Jeans mass M_J) on the gas fraction suppression in low mass objects has the same appearance as the non-expanding universe with the reheating temperature of only a few thousand degrees.

For most practical applications the knowledge of $\bar{M}_g(M_t, t)$ may be sufficient, but the resolution of my simulations is also sufficient to approximately characterize the whole distribution function $P(M_g, M_t)$. Using the product rule of probability theory, this distribution function can be written as the product of the probability to find an object with the total mass M_t and the probability distribution of the gas masses for all objects with a given total mass,

$$P(M_g, M_t) = P(M_t)P(M_g|M_t).$$

The former probability depends on the cosmological model, whereas the latter may be conjectured to be independent of the specific model, and depend only on the characteristic mass scales present at this moment. The physical reason for this conjecture is simple: the number density of cosmological objects of a given mass depends on the cosmological model, but as long as this number density is not exceedingly high, different objects as virialized entities are independent of each other and the rest of the universe, and thus a probability for an object to lose a given fraction of its gas mass should not depend strongly on the abundance of other objects somewhere else in the universe.

The number of objects in the simulations is not high enough to accurately measure the probability distribution function $P(M_g|M_t)$, but it appears that for any M_t and at any given time this distribution is compatible with a lognormal distribution. Assuming that it is indeed lognormal, I can write it down as follows:

$$P(M_g|M_t) = \frac{1}{\sigma \sqrt{2\pi}} \exp \left[-\frac{1}{2\sigma^2} \left(\ln M_g - \ln \bar{M}_g + \sigma^2/2 \right)^2 \right], \quad (10)$$

where σ is the rms dispersion of the logarithm of the gas mass, and is a function of the total mass, as is \bar{M}_g (eq. [8]).

In order to come up with a closed form fitting formula, I approximate σ by the following power-law:

$$\sigma(M_t) = \frac{M_C^*}{3M_t},$$

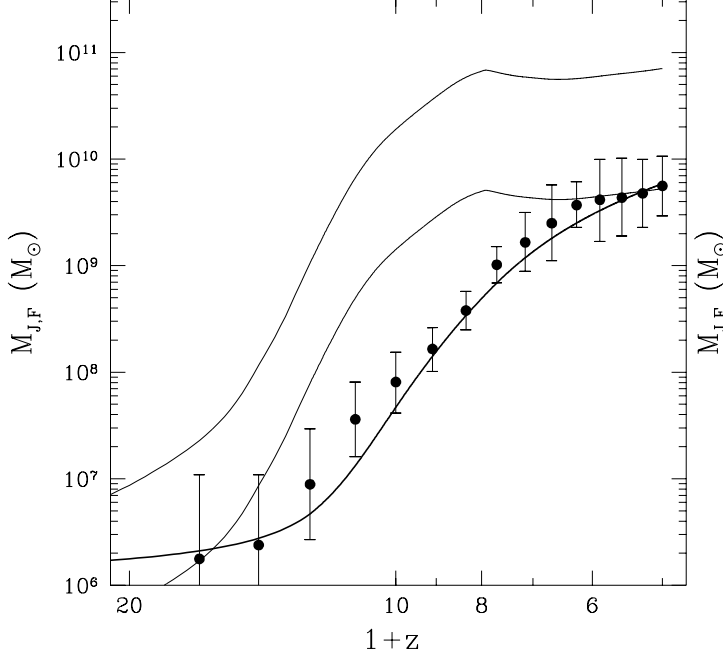


Fig. 4a

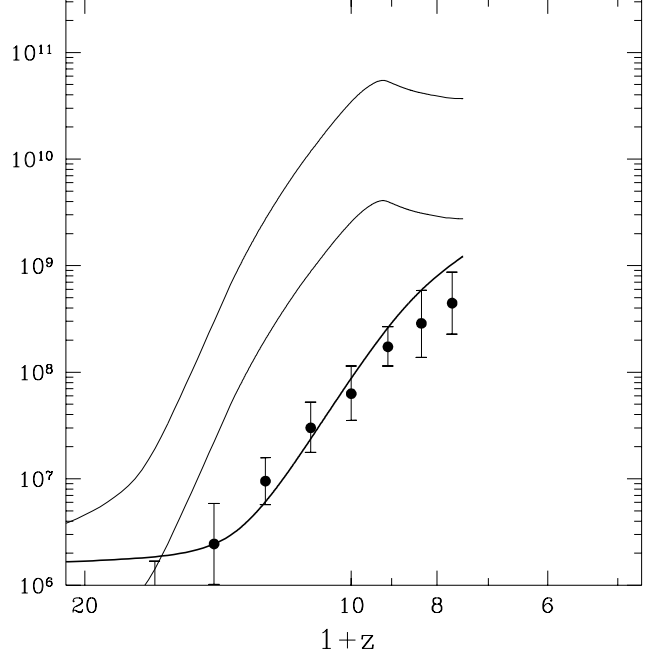


Fig. 4b

Fig. 4.— The same as Fig. 3, except that the symbols now show the characteristic mass M_C^* from the fitting formula for the rms dispersion σ of the lognormal distribution $P(M_g|M_t)$ at a given M_t .

where M_C^* is another characteristic mass, which is plotted in Figure 4 together with the Jeans mass and the filtering mass. Again, as one can see, the characteristic mass M_C^* is approximately equal to the filtering mass, so that the rms dispersion of the logarithm of gas mass at a given total mass is given by the following fit:

$$\sigma(M_t, t) \approx \frac{M_F(t)}{3M_t}. \quad (11)$$

The last equation is not very well constrained by my simulations. For example, the coefficient in the denominator is determined with only 30% accuracy, so replacing it with 2 or 4 also gives an acceptable fit to the data.

Equations (8-11) give in a closed form the probability distribution function $P(M_g|M_t, t)$ for any cosmological model and reionization history (which are specified through the filtering mass $M_F(t)$ as a function of time).

4. Low Redshift Evolution

Given the thermal history of the universe, the evolution of the linear theory Jeans mass and thus the filtering mass can be calculated up to the present time. In a universe with a single (hydrogen) reionization epoch the temperature at late times is theoretically predicted to

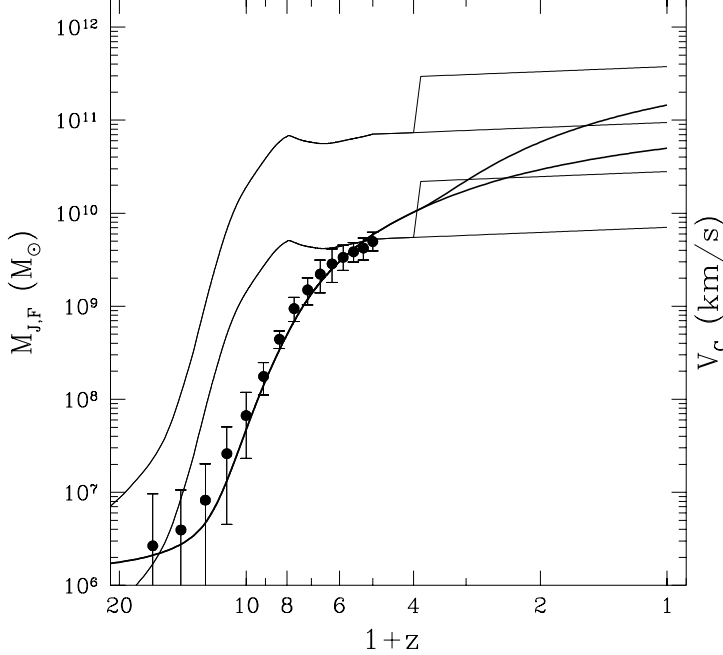


Fig. 5a

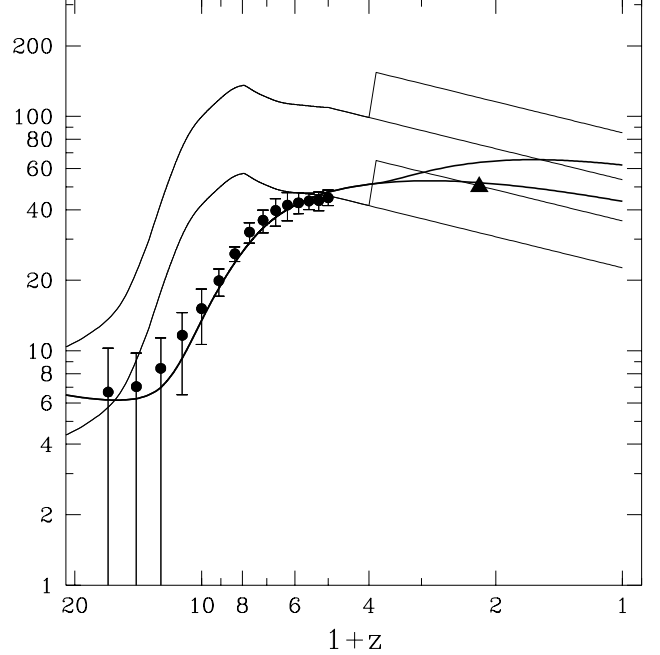


Fig. 5b

Fig. 5.— (a) Extrapolation of Fig. 3a to $z = 0$. Lower solid curves show the extrapolation assuming the temperature evolution $T \propto a^{-0.88}$, whereas the upper curves also include a second reheating at $z = 3$ as indicated by the observations. (b) The same plot with masses converted into circular velocities. The triangle shows the results of Thoul & Weinberg (1996) and Quinn et al. (1996) for the model without reheating (lower solid curves).

evolve as $\propto a^{-0.88}$ (Miralda-Escudé & Rees 1994; Hui & Gnedin 1997). However, recent analyses of Lyman-alpha forest data indicate that the universe underwent a second reheating at $z \approx 3$ (Ricotti, Gnedin, & Shull 2000; Schaye et al. 2000), possibly as the result of helium reionization by quasars. In order to account for it, I also consider a thermal history for which the gas temperature is increased sharply at $z = 3$ by a factor of 2.5. Figure 5 shows the predicted evolution of the filtering mass, the linear theory Jeans mass, and the Jeans mass at the virial overdensity for the two cases (the upper curves correspond to the secondary reheating model) in an $\Omega_0 = 1$ universe (for a flat universe with the cosmological constant, the result is almost indistinguishable). This paper therefore makes a prediction that objects as massive as $10^{11} M_\odot$ have on average a baryon fraction of only 50% of the universal value. (The baryonic content of these objects is likely to be dominated by stars at the present time.) Note, however, that in terms of circular velocities, the characteristic scale is essentially independent of redshift, and is about 50 km/s, in agreement with previous investigations (Thoul & Weinberg 1996; (Quinn, Katz, & Efstathiou 1996; Weinberg, Hernquist, & Katz 1997). The Jeans mass at the virial overdensity is, however, a decreasing function of time, and corresponds to a circular velocity of only about 30 km/s at $z = 2$ in the model without the secondary reheating, contrary to the numerical results. This gives a further

illustration of the fact that the Jeans mass (at any overdensity) is not the proper scale that controls the gas fraction in low mass objects.

5. Conclusions

Based on cosmological simulation of reionization, I showed that the linear Jeans mass does not control the mass scales over which reionization suppresses the gas fraction in low mass cosmological objects, and may overestimate the characteristic mass scale by an order of magnitude. Since the Jeans mass is a function of the density, at the virial overdensity of 180 the Jeans mass is able to match the characteristic scale at later times, but the general shape of the Jeans mass vs redshift and the characteristic mass vs redshift do not match. Instead, the filtering mass, which directly corresponds to the length scale over which the baryonic perturbations are smoothed in linear theory, provides a good fit to the characteristic mass scale. This conclusions supports a very simple picture (proposed by Shapiro et al. 1994) in which the effect of reionization on structure formation in the universe is controlled by a single mass scale both in the linear and the nonlinear regime. However, this work demonstrates that it is not the Jeans mass (as was previously thought) but the filtering mass that is the appropriate mass scale.

The distribution of the gas fractions of all cosmological objects with the same total mass at any given moment during the evolution of the universe is approximately lognormal, is fully specified by the filtering mass at this moment, and is given by equations (8-11).

These equations, supplemented with the total-mass function of cosmological objects, fully describe the full probability distribution to find an object with given values of its gas and total mass. This probability distribution can be conveniently used in semi-analytical modeling of the evolution of low mass objects in the universe.

Admittedly, the simulations used in this paper consider only one cosmological model, but all cosmological models (including those that are curvature- or vacuum-dominated today) have an expansion law that approaches $a \propto t^{2/3}$ at sufficiently high redshift, and follow similar behavior. Thus, while the applicability of equations (8-11) for a wide range of cosmological models is not rigorously proven, the physical reasoning suggests that this is likely to be the case.

My simulations also do not cover all the possible reionization histories, but at least runs A and B have different reionization histories and different resolutions, which gives some credibility to the conjecture that equations (8-11) work for different reionization histories and are also free from numerical artifacts.

I am grateful to the referee David Weinberg for fruitful comments that substantially improved the original manuscript. This work was partially supported by National Computational Science Alliance under grant AST-960015N and utilized the SGI/CRAY Origin 2000 array at the National

Center for Supercomputing Applications (NCSA).

REFERENCES

Babul, A., & Rees, M. J. 1992, MNRAS, 255, 346

Bertschinger, E., & Gelb, J. 1991, J. Comput. Phys., 5, 164

Efstathiou, G. 1992, MNRAS, 256, 43P

Gnedin, N. Y. 1995, ApJS, 97, 231

Gnedin, N. Y. 1996, ApJ, 456, 1

Gnedin, N. Y. 2000, ApJ, in press (astro-ph/9909383)

Gnedin, N. Y., & Bertschinger, E. 1996, ApJ, 470, 115

Gnedin, N. Y., & Hui, L. 1998, MNRAS, 296, 44

Haiman, Z., Thoul, A. A., & Loeb, A. 1996, ApJ, 464, 523

Hui, L., & Gnedin, N. Y. 1997, MNRAS, 292, 27

Ikeuchi, S. 1986, Ap&SS, 118, 509

Miralda-Escudé, J., & Rees, M. J. 1994, MNRAS, 266, 343

Navarro, J., & Steinmetz, M. 1997, ApJ, 478, 13

Quinn, T., Katz, N., & Efstathiou, G. 1996, ApJ, 278, 49P

Rees, M. J. 1986, MNRAS, 218, 25P

Ricotti, M., Gnedin, N. Y., & Shull, J. M. 2000, ApJ, in press (astro-ph/9906413)

Schaye, J., Theuns, T., Rauch, M., Efstathiou, G., & Sargent, W. L. W. 2000, MNRAS, submitted (astro-ph 9912432)

Shapiro, P. R., Giroux, M. L., & Babul, A. 1994, ApJ, 427, 25

Thoul, A. A., & Weinberg, D. H. 1996, ApJ, 465, 608

Weinberg, D. H., Hernquist, L., & Katz, N. 1997, ApJ, 477, 8